

Natriuretic Peptides/cGMP/cGMP-Dependent Protein Kinase Cascades Promote Muscle Mitochondrial Biogenesis and Prevent Obesity

Kazutoshi Miyashita,¹ Hiroshi Itoh,¹ Hirokazu Tsujimoto,² Naohisa Tamura,² Yasutomo Fukunaga,² Masakatsu Sone,² Kenichi Yamahara,² Daisuke Taura,² Megumi Inuzuka,² Takuhiro Sonoyama,² and Kazuwa Nakao²

OBJECTIVE—Natriuretic peptides (NPs) have been characterized as vascular hormones that regulate vascular tone via guanylyl cyclase (GC), cyclic GMP (cGMP), and cGMP-dependent protein kinase (cGK). Recent clinical studies have shown that plasma NP levels were lower in subjects with the metabolic syndrome. The present study was conducted to elucidate the roles for NP/cGK cascades in energy metabolism.

RESEARCH DESIGN AND METHODS—We used three types of genetically engineered mice: brain NP (BNP) transgenic (BNP-Tg), cGK-Tg, and guanylyl cyclase-A (GCA) heterozygous knockout ($GCA^{+/-}$) mice and analyzed the metabolic consequences of chronic activation of NP/cGK cascades in vivo. We also examined the effect of NPs in cultured myocytes.

RESULTS—BNP-Tg mice fed on high-fat diet were protected against diet-induced obesity and insulin resistance, and cGK-Tg mice had reduced body weight even on standard diet; surprisingly, giant mitochondria were densely packed in the skeletal muscle. Both mice showed an increase in muscle mitochondrial content and fat oxidation through upregulation of peroxisome proliferator-activated receptor (PPAR)- γ coactivator (PGC)-1 α and PPAR δ . The functional NP receptors, GCA and guanylyl cyclase-B, were downregulated by feeding a high-fat diet, while $GCA^{+/-}$ mice showed increases in body weight and glucose intolerance when fed a high-fat diet. NPs directly increased the expression of PGC-1 α and PPAR δ and mitochondrial content in cultured myocytes.

CONCLUSIONS—The findings together suggest that NP/cGK cascades can promote muscle mitochondrial biogenesis and fat oxidation, as to prevent obesity and glucose intolerance. The vascular hormone, NP, would contribute to coordinated regulation of oxygen supply and consumption. *Diabetes* 58: 2880–2892, 2009

From the ¹Department of Internal Medicine, School of Medicine, Keio University, Tokyo, Japan; and the ²Department of Medicine and Clinical Science, Kyoto University Graduate School of Medicine, Kyoto, Japan.

Corresponding author: Hiroshi Itoh, hrith@sc.itc.keio.ac.jp.

Received 15 March 2009 and accepted 28 July 2009. Published ahead of print at <http://diabetes.diabetesjournals.org> on 18 August 2009. DOI: 10.2337/db09-0393.

© 2009 by the American Diabetes Association. Readers may use this article as long as the work is properly cited, the use is educational and not for profit, and the work is not altered. See <http://creativecommons.org/licenses/by-nc-nd/3.0/> for details.

The costs of publication of this article were defrayed in part by the payment of page charges. This article must therefore be hereby marked "advertisement" in accordance with 18 U.S.C. Section 1734 solely to indicate this fact.

See accompanying commentary, p. 2726.

Natriuretic peptides (NPs), consisting of atrial, brain, and C-type NPs (ANP, BNP, and CNP, respectively), have been characterized as cardiac or vascular hormones that reduce vascular tone and circulating blood volume (1). NPs can stimulate at least two types of biologically active receptors, guanylyl cyclase-A (GCA) and guanylyl cyclase-B (GCB), which act as membrane-bound GCs to synthesis intracellular cGMP. NPs exert their biological effects through GC-mediated synthesis of cyclic GMP (cGMP) and subsequent activation of cGMP-dependent protein kinase (cGK)-I, which constitute the common signal transduction pathway for nitric oxide (NO). On the other hand, type C NP receptor (C-receptor) is indicated as having a role as a clearance receptor, which binds and incorporates NPs into cytoplasm and inactivates them.

We and others (2) have demonstrated that the intravenous infusion of ANP or BNP into patients with heart failure reduces cardiac pre- and post-load and results in beneficial hemodynamic function; therefore, they are widely used for the treatment of congestive heart failure. Recently, we have elucidated new roles for NPs in the promotion of neovascularization in ischemic tissues and introduced a therapeutic application of NPs for patients with peripheral artery occlusive diseases (3,4). Meanwhile, CNP is shown to stimulate endochondral bone formation through GCB-dependent signal pathways, and its therapeutic application to human achondroplasia is expected (5).

In these ways, the cardiac hormones, NPs, have been indicated to act on the cardiovascular and cartilage-bone systems. Recent reports have suggested that NPs may also affect cultured human adipocytes and exert lipolytic action (6), which is associated with cGK-mediated activation of hormone-sensitive lipase (HSL) (7). In addition, obese individuals in the cohorts of the Framingham Heart Study were found to hold considerably lower plasma NP levels than those with normal weight (8). Lower plasma NP levels were also associated with the development of insulin resistance and metabolic syndrome, even after adjustment for BMI (9). These findings indicate that the activation of NP/cGK cascades can regulate lipid metabolism in humans to reduce susceptibility to obesity and the metabolic syndrome.

In a previous report (10), we have shown that cGMP can regulate mitochondrial content and function in C2C12 myotubular cells by altering the expressions of genes involved in mitochondrial biogenesis and reactive oxygen

species production. In the present study, we analyzed three types of genetically engineered mice to elucidate the metabolic consequences of chronic activation of NP/cGK cascades in vivo. One type is BNP transgenic mice (BNP-Tg) with serum amyloid P (SAP) promoter, which overexpress BNP specifically in the liver and have BNP plasma levels 100 times higher than the physiological condition (11). The other two types are cGK transgenic mice (cGK-Tg) with a chicken β -actin promoter combined with cytomegalovirus immediate-early enhancers (CAG promoter), which overexpress human cGK-I ubiquitously (3), and GCA heterozygous knockout (GCA^{+/-}) mice (12). The findings of the present study demonstrate significant roles for NP/cGK cascades in mitochondrial biogenesis, fat oxidation, and oxygen consumption, indicating that an activation of the cascades would be therapeutically beneficial for the treatment of obesity, insulin resistance, fatty liver, and the metabolic syndrome.

RESEARCH DESIGN AND METHODS

RESEARCH DESIGN AND METHODS are shown in supplement 1 in the online appendix (13–16) (available at <http://diabetes.diabetesjournals.org/cgi/content/full/db09-0393/DC1>).

RESULTS

BNP-Tg mice attenuate diet-induced obesity and insulin resistance. To examine the effects of NPs on body weight and on glucose and lipid metabolism, BNP-Tg mice were given a high-fat (60 kcal% fat) diet. The body weight of BNP-Tg mice on standard diet tended to decrease compared with that of their littermate wild-type mice (4.8% reduction at 18 weeks old, $n = 18$ per group, $P = 0.06$) (Fig. 1A). When fed a high-fat diet from the age of 10 weeks, on the other hand, the weight of the BNP-Tg mice at 18 weeks old was significantly lower than that of the wild-type controls (38.9 ± 1.0 g for the former and 43.0 ± 0.9 g for the latter; $n = 10$, $P < 0.01$) (Fig. 1A). The reduction in body weight of the transgenic mice fed a high-fat diet could be macroscopically observed (Fig. 1B). Food intake (kcal/day) was not significantly different between BNP-Tg and wild-type mice whether on standard or high-fat diet, despite the difference in body weight (Fig. 1C).

The blood glucose and insulin levels were identical for BNP-Tg and wild-type mice on standard diet, both during ad libitum feeding and fasting. However, these levels were significantly lower in BNP-Tg mice during ad libitum feeding of the high-fat diet (Table 1). Blood glucose levels were also lower in BNP-Tg mice fed a high-fat diet after administration of glucose or insulin (Fig. 1D). On the other hand, serum triglyceride and fatty acid levels did not show any significant differences between the two groups, both when feeding ad libitum and fasting (Table 1). The greater increase in the serum fatty acid level after 24-h fasting was observed in BNP-Tg mice (Table 1). Urinary excretion of catecholamines (epinephrine and norepinephrine) was similar between the two groups (Table 1).

To estimate the fat weight in mice, we used computed tomography (CT) and scanned the whole body of mice. The high-fat diet produced a substantial increase in the adipose tissue in both the subcutaneous and visceral area. The total fat weight of BNP-Tg mice fed on a high-fat diet was significantly lower (26% reduction, $n = 6$, $P < 0.01$) (Fig. 1E) than that of wild-type mice. The relative reduction ratio was similar for both subcutaneous and visceral fat (21% reduction for subcutaneous and 29% for visceral

fat). The high-fat-fed BNP-Tg mice had less surgically harvested epididymal and visceral fats than the wild-type mice (Fig. 1F), which is a compatible finding with the CT-based fat quantification. On the other hand, lean body mass showed no significant difference (26.6 ± 1.3 g in BNP-Tg mice fed a high-fat diet and 27.2 ± 1.2 g in wild-type mice).

To further study the effects of NPs on diet-induced lipid accumulation, we examined adipose tissue, liver, and skeletal muscle of BNP-Tg mice fed a high-fat diet for a comparison with those of wild-type mice. We found that the histologically examined adipocytes in the epididymal fat were smaller in BNP-Tg mice (Fig. 1G). In support of this finding, serum leptin was found to decrease and adiponectin to increase in BNP-Tg mice fed a high-fat diet (Fig. 1H). The liver of wild-type mice had a whitish appearance, while that of high-fat-fed BNP-Tg mice was reddish and lower in weight (1.4 ± 0.1 g in high-fat-fed BNP-Tg mice and 1.7 ± 0.1 g in wild-type mice, $n = 6$, $P < 0.05$) (Fig. 1I). Oil red O staining and triglyceride measurements of the liver confirmed that diet-induced lipid accumulation was significantly attenuated in high-fat-fed BNP-Tg mice (30% decrease in triglyceride concentration, $P < 0.05$, $n = 12$) (Fig. 1J), and a similar attenuation of lipid accumulation was observed in the skeletal muscle (27% reduction, $n = 12$, $P < 0.05$) (Fig. 1K). These findings indicate that diet-induced ectopic fat accumulation was reduced in BNP-Tg mice in addition to the reduction in adipose tissue.

High-fat-fed BNP-Tg mice exhibit higher oxygen consumption and fat oxidation. The respiratory gas analysis demonstrated that BNP-Tg mice on a high-fat diet consumed more oxygen than wild-type mice ($n = 6$, $P < 0.01$) (Fig. 2A). Mean oxygen consumption for 24 h of BNP-Tg mice on standard diet was 64.3 ± 0.9 ml \cdot min⁻¹ \cdot kg body wt⁻¹, and that of wild-type mice was 62.6 ± 0.9 ml \cdot min⁻¹ \cdot kg body wt⁻¹. The value of wild-type mice on high-fat diet decreased to 51.8 ± 0.7 ml \cdot min⁻¹ \cdot kg body wt⁻¹, and that of BNP-Tg was 58.7 ± 0.5 ml \cdot min⁻¹ \cdot kg body wt⁻¹. The value was significantly higher than that of wild-type mice ($n = 6$, $P < 0.01$) (Fig. 2B). The rectal temperature was similar between BNP-Tg and wild-type mice, whether on standard diet or high-fat diet (Fig. 2C). The respiratory quotient showed a significant reduction in high-fat-fed BNP-Tg mice, especially during the daytime (Fig. 2D). The mean respiratory quotient for 24 h of high-fat-fed BNP-Tg mice was 0.80 ± 0.02 , and that of wild-type mice was 0.81 ± 0.01 ($n = 6$, $P < 0.05$). In line with the reduction in respiratory quotient, mean fat oxidation for 24 h of high-fat-fed BNP-Tg mice, estimated from the results of the respiratory gas analysis, was increased to 18.5 ± 0.2 ml \cdot min⁻¹ \cdot kg body wt⁻¹, while that of wild-type mice was 16.8 ± 0.2 ml \cdot min⁻¹ \cdot kg body wt⁻¹ ($n = 6$, $P < 0.01$) (Fig. 2E). The increase in fat oxidation in BNP-Tg mice could be augmented by fasting (Fig. 2F).

To further investigate the mechanism for the increase in oxygen consumption of high-fat-fed BNP-Tg mice, we checked mitochondrial DNA copy number in the brown adipose tissue and skeletal muscle, which are the major sites for energy expenditure. Quantitative PCR analysis demonstrated a significant increase in the mitochondrial DNA copy number in the skeletal muscle of high-fat-fed BNP-Tg mice (Fig. 2G); however, the increase in the brown adipose tissue was weak (Fig. 2G), in accordance with unchanged rectal temperature (Fig. 2C). In conjunction with these findings, the expressions of the genes encoding peroxisome proliferator-activated receptor (PPAR)- γ coactivator (PGC)-1 α and un-

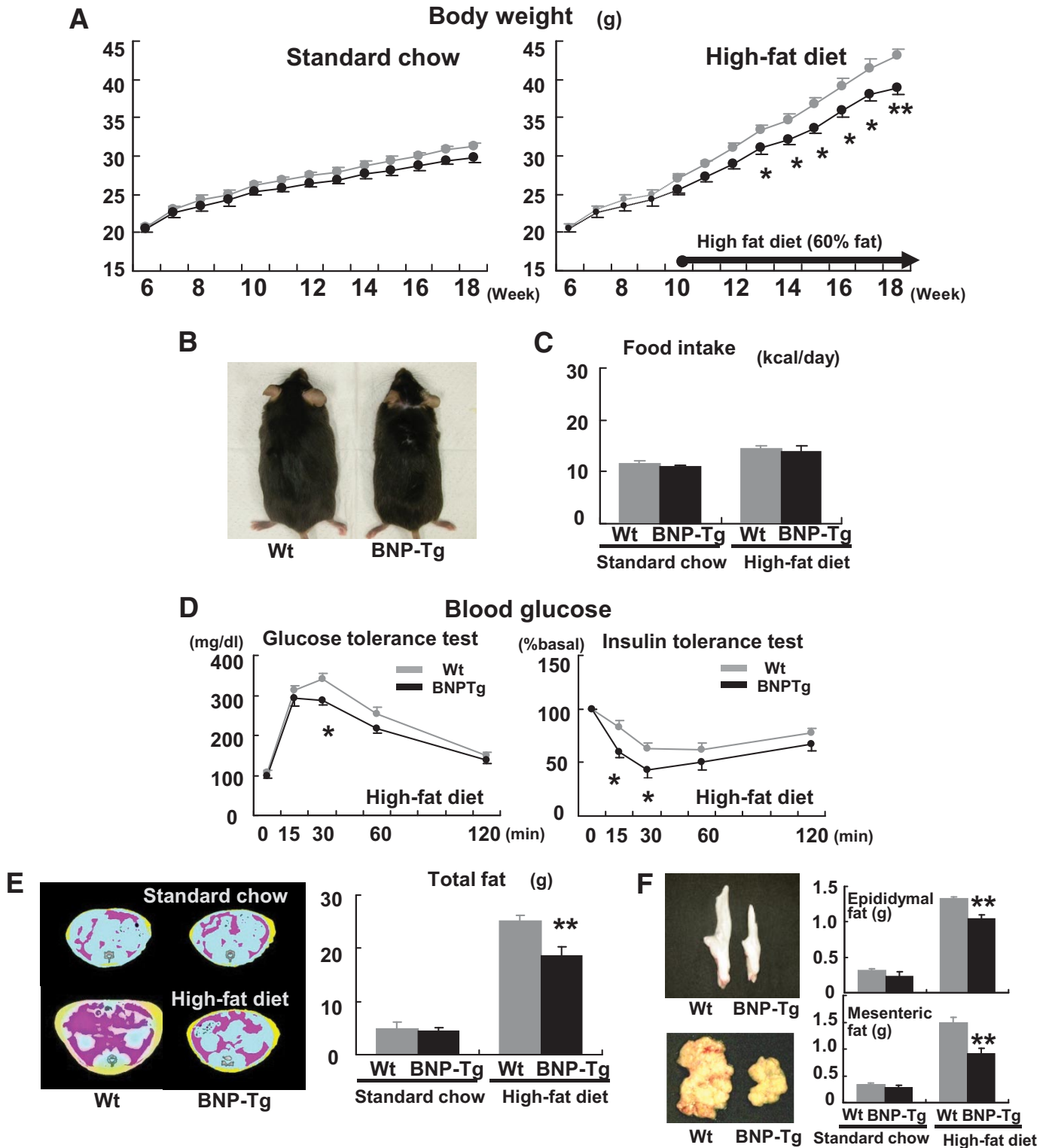


FIG. 1. BNP-Tg mice are protected against diet-induced obesity and insulin resistance. Wild-type and BNP-Tg mice were given high-fat (60 kcal% fat) diet from the age of 10 weeks. **A:** Body weight of the BNP-Tg mice on standard diet (*left panel*) and a high-fat diet (*right panel*) ($n = 18$ per group on standard diet and $n = 10$ on high-fat diet). □, wild type; ■, BNP-Tg. **B:** Macroscopic appearance of a wild-type (Wt) and a BNP-Tg mouse fed on high-fat diet at 18 weeks of age. **C:** Food intake on standard diet and high-fat diet ($n = 6$). **D:** Blood glucose levels determined with the glucose and insulin tolerance tests ($n = 8$). □, wild type; ■, BNP-Tg. **E:** CT images obtained at kidney level of a wild-type (Wt) and a BNP-Tg mouse on standard diet (*upper panel*) and high-fat diet (*lower panel*). Subcutaneous fat (yellow), abdominal fat (red), and muscular region (blue) were distinguished. Total fat weight was estimated from the images ($n = 6$). **F:** Macroscopic appearances and weights of epididymal fat (*upper panel*) and mesenteric fat (*lower panel*). **G:** Microscopic analysis with hematoxylin and eosin staining of epididymal fat in high-fat-fed mice (*left panels*). Scale bar, 100 μ m. Adipocyte size of epididymal fat in high-fat-fed mice was estimated from the histological analysis (*right panel*) ($n = 8$). **H:** Serum leptin and adiponectin levels ($n = 8$). **I:** Macroscopic appearance of the liver of the mice fed on high-fat diet (*upper panel*). Microscopic images of the liver stained with Oil red O (*lower panel*). Scale bar, 100 μ m. **J** and **K:** Triglyceride concentrations in the liver (**J**) and the quadriceps (**K**) ($n = 12$). * $P < 0.05$; ** $P < 0.01$ vs. wild-type (Wt) mice on the same feeding condition. (A high-quality color digital representation of this figure is available in the online issue.)

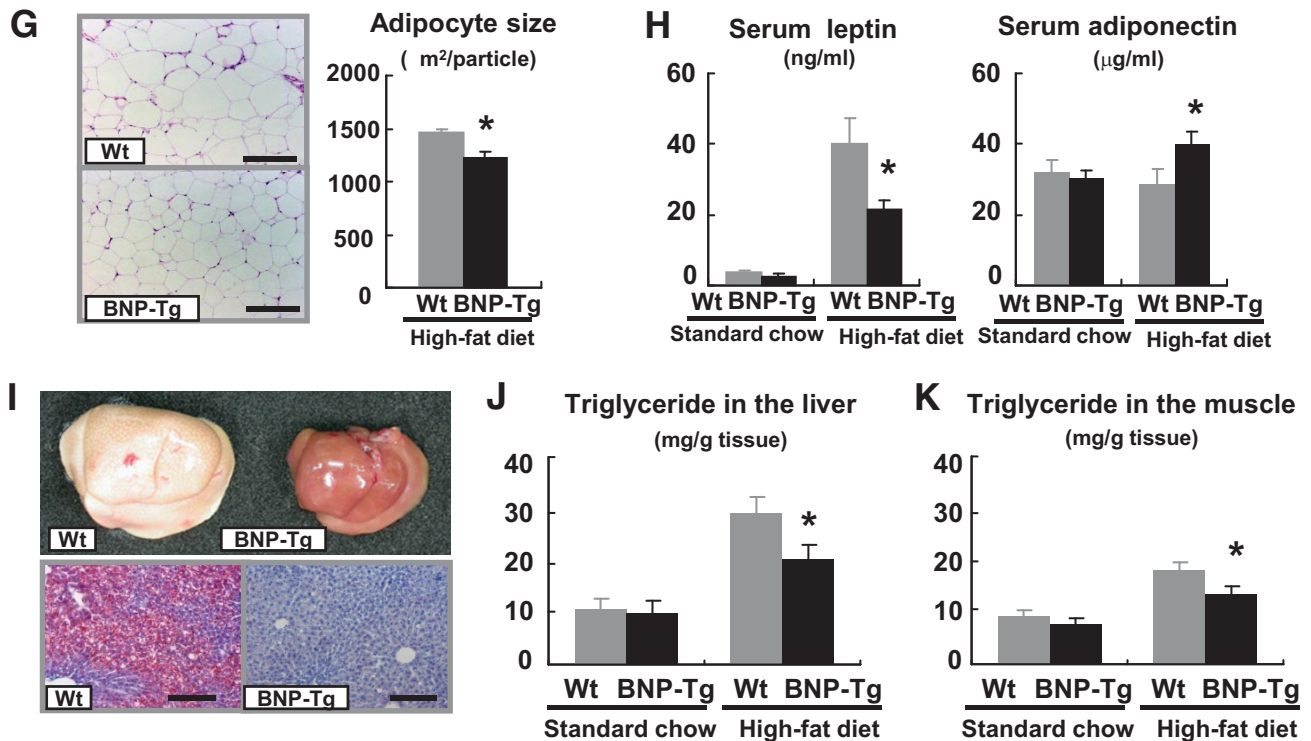


FIG. 1. Continued.

coupling protein (UCP) 1, which are known to mediate mitochondrial biogenesis and thermogenesis, respectively, were not significantly upregulated in the brown adipose tissue of the Tg mice (Fig. 2H); whereas in the skeletal muscle, the expressions of the genes encoding PGC-1 α and PPAR δ , which are known to participate in fat oxidation and energy expenditure, were upregulated in high-fat-fed BNP-Tg mice (Fig. 2H).

The expressions of NP receptors are regulated by feeding condition, and GCA knockdown mice are susceptible to diet-induced obesity and glucose intolerance. The results of the study shown in Fig. 3 are described in supplement 2 in the online appendix.

TABLE 1
Physical and metabolic parameters of high-fat-fed BNP-Tg mice

	Wild type	BNP-Tg
Body weight (g)		
18 weeks old	43.0 \pm 0.9	38.9 \pm 0.9*
Glucose (mg/dl)		
Ad libitum feeding	230.2 \pm 10.5	196.7 \pm 16.5 \dagger
24-h fasting	135.9 \pm 7.9	104.0 \pm 10.2 \dagger
Insulin (ng/dl)		
Ad libitum feeding	9.87 \pm 1.9	5.25 \pm 1.1 \dagger
24-h fasting	1.05 \pm 0.2	0.86 \pm 0.1
Triglyceride (mg/dl)		
Ad libitum feeding	131.9 \pm 13.2	126.7 \pm 15.6
24-h fasting	90.9 \pm 7.9	92.6 \pm 8.8
Fatty acid (mEq/l)		
Ad libitum feeding	1.28 \pm 0.10	1.08 \pm 0.09
24-h fasting	1.70 \pm 0.17	1.75 \pm 0.21
Epinephrine (ng/day)		
Urinary excretion	26.5 \pm 2.9	28.0 \pm 4.2
Norepinephrine (ng/day)		
Urinary excretion	358.0 \pm 15.1	349.0 \pm 52.8

* $P < 0.01$, $\dagger P < 0.05$, compared with wild type.

cGK-Tg mice are lean and insulin sensitive even on standard diet. To determine the effect of cGK-I, a major downstream effector of NP/GC/cGMP cascades, on body weight and on glucose and lipid metabolism, we examined the cGK-Tg mice with ubiquitously overexpressing human cGK-I. The cGK-Tg mice showed a significant reduction in body weight compared with wild-type mice, even on standard diet (27.6 \pm 0.4 g for cGK-Tg and 32.0 \pm 0.6 g for wild-type mice, at 18 weeks old on standard diet, $n = 8$, $P < 0.01$) (Fig. 4A). Moreover, high-fat diet-induced weight gain was attenuated in the Tg mice, and the reduction in body weight eventually reached >20%. At 18 weeks of age, their body weight was 35.7 \pm 0.4 g, and that of wild-type mice was 43.9 \pm 0.6 g (after 8 weeks of high-fat feeding, $n = 8$, $P < 0.01$) (Fig. 4A and B). The daily food intake (kcal/day) was not noticeably different for cGK-Tg and wild-type mice, while it showed a significant increase in cGK-Tg mice when it was adjusted for body weight (kcal \cdot day⁻¹ \cdot g body wt⁻¹) (Fig. 4C).

The blood glucose levels were significantly lower in cGK-Tg mice, both during ad libitum feeding and fasting and on standard diet and high-fat diet (Table 2). The decrease was accompanied by significantly lower insulin levels (Table 2), except for the value for fasting while fed on standard diet. After administration of glucose or insulin, the difference in glucose levels between cGK-Tg and wild-type mice became more prominent (Fig. 4D). Serum triglyceride and fatty acid levels were similar for cGK-Tg and wild-type mice, both during ad libitum feeding and fasting, except for the significant increase in fatty acid levels in high-fat-fed cGK-Tg mice during fasting, when compared with that of wild-type mice (Table 2). Urinary excretion of the catecholamines (epinephrine and norepinephrine) was similar for wild-type and cGK-Tg mice (Table 2).

In parallel with the reduction in body weight, fat tissues assessed by means of CT analysis were significantly reduced

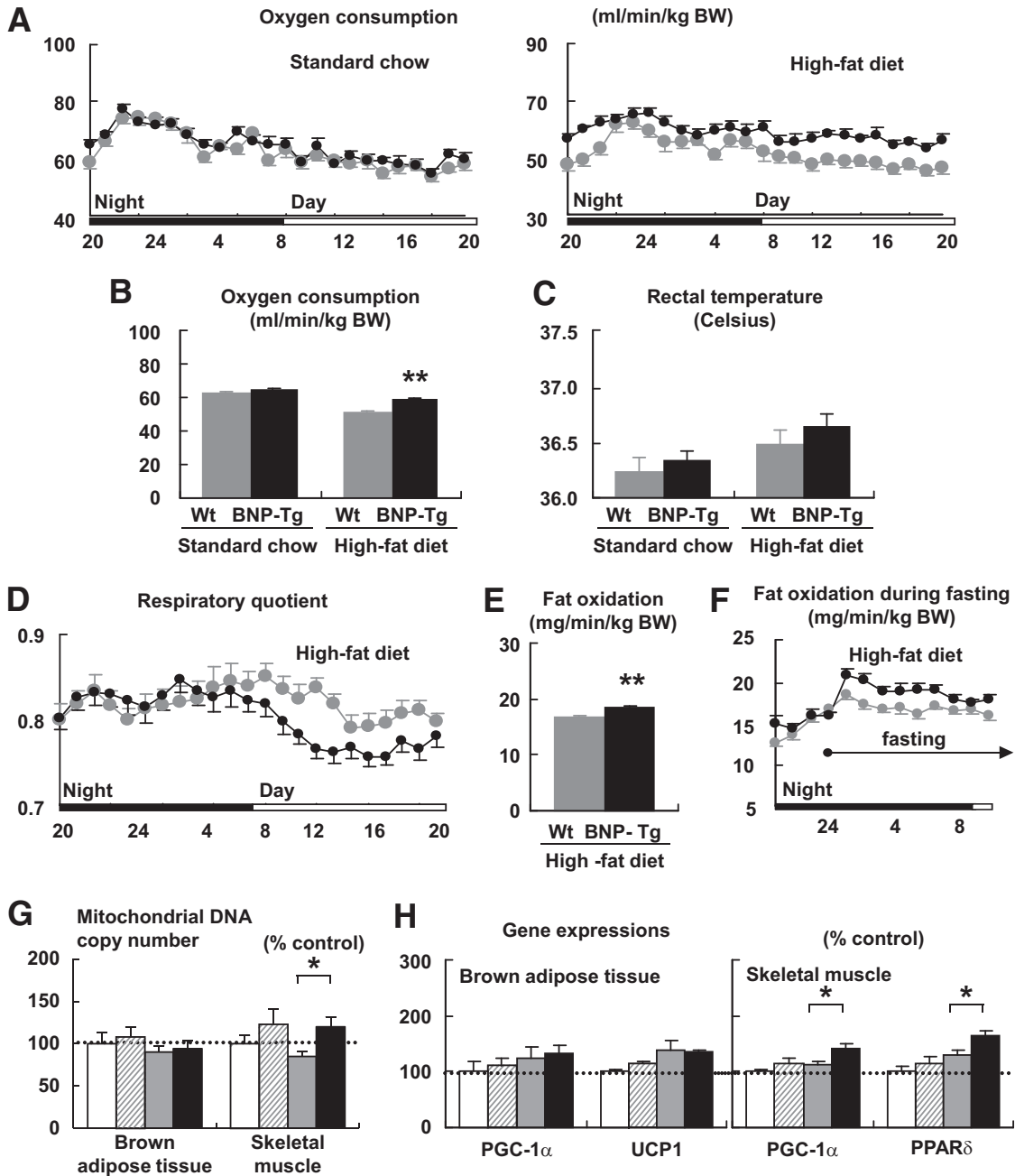


FIG. 2. High-fat-fed BNP-Tg mice exhibit higher oxygen consumption and fat oxidation in association with increased mitochondrial content in the skeletal muscle. Mice were subjected to respiratory gas analysis after fed on high-fat diet. Total DNA and RNA were extracted from the brown adipose tissue and the quadriceps, and quantitative PCR analysis was performed. *A:* Oxygen consumption on standard diet (*left panel*) and high-fat diet (*right panel*) ($n = 6$). □, wild type; ■, BNP-Tg. *B:* Mean oxygen consumption for 24 h on standard diet or high-fat diet ($n = 6$). *C:* Rectal temperature on standard diet or high-fat diet ($n = 6$). *D:* Respiratory quotient of high-fat-fed mice ($n = 6$). □, wild type; ■, BNP-Tg. *E:* Mean fat oxidation estimated from the respiratory gas analysis for 24 h of high-fat-fed mice. *F:* Fat oxidation before and during fasting starting from midnight. □, wild type; ■, BNP-Tg. *G:* Mitochondrial DNA copy number estimated from quantification of mitochondrial and nuclear genome ($n = 8$). *H:* Expressions of genes encoding PGC-1 α and UCP1 in the brown adipose tissue and those for PGC-1 α and PPAR δ in the skeletal muscle ($n = 8$). Standard diet: □, wild type; ▨, BNP-Tg. High-fat diet: □, wild type; ■, BNP-Tg. The values were standardized to those for the control (wild-type [Wt] mice fed on standard diet) in either group. * $P < 0.05$; ** $P < 0.01$ vs. wild type on the same feeding condition.

in cGK-Tg mice, both on standard and high-fat diet (Fig. 4E). Hematoxylin-eosin staining and the Coulter counter analysis showed that the adipocytes in the epididymal fat were smaller in cGK-Tg mice, with mean adipocyte diameters for wild-type and cGK-Tg mice of ~ 80 and $60 \mu\text{m}$, respectively, when on standard diet (Fig. 4F and G). The high-fat diet produced an increase in the diameter to $130 \mu\text{m}$ in wild-type mice but to only $80 \mu\text{m}$ in the Tg mice (Fig. 4G). The liver of high-fat-fed cGK-Tg mice weighed less than that of wild-type

mice ($1.3 \pm 0.1 \text{ g}$ and $1.8 \pm 0.1 \text{ g}$, $n = 8$, $P < 0.01$, respectively) and had reddish appearance (Fig. 4H). The hepatic triglyceride concentration of high-fat-fed cGK-Tg mice was significantly reduced when compared with wild-type mice (30% decrease at 20 weeks, $n = 6$, $P < 0.05$) (Fig. 4I). Muscular triglyceride concentration of cGK-Tg mice was also significantly lower, even on standard diet, as well as in high-fat-fed cGK-Tg mice (44% decrease in muscle triglyceride at 20 weeks, $n = 6$, $P < 0.01$) (Fig. 4J).

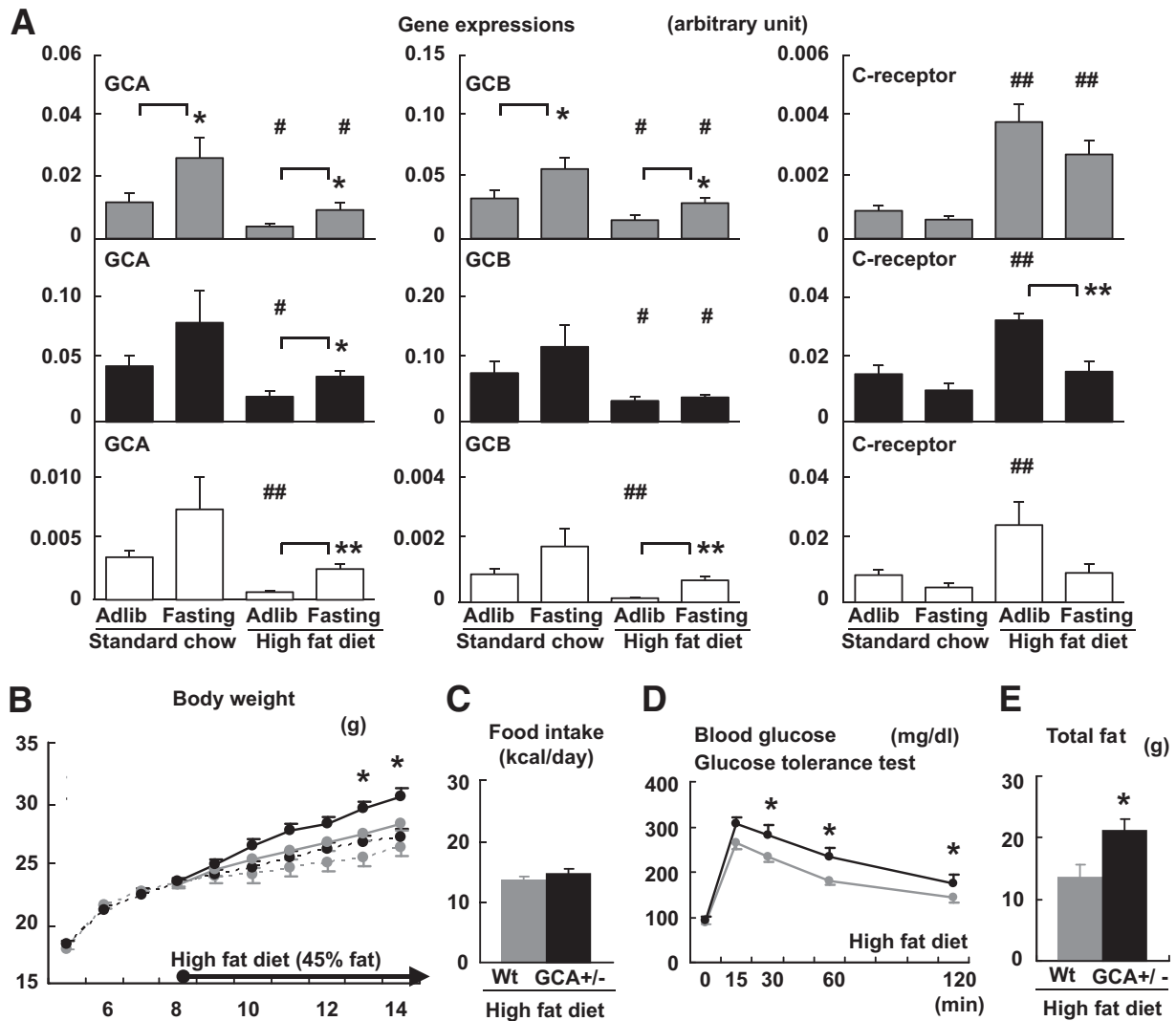


FIG. 3. The expressions of NP receptors are regulated by feeding condition, while GCA knockdown mice are susceptible to diet-induced obesity and glucose intolerance. Total RNA was extracted from the quadriceps of wild-type mice, and quantitative PCR analysis for the expressions of NP receptors was performed. Wild-type and GCA heterozygous knockout mice (GCA^{+/-}) were given a high-fat (45 kcal% fat) diet from the age of 8 weeks. **A:** Expressions of GCA, GCB, and C-receptor in the skeletal muscle, brown adipose tissue, and white adipose tissue of wild-type mice for indicated feeding condition ($n = 8$). The values represent the expression levels of each gene compared with that of β -actin determined by quantitative PCR analysis. Statistical analysis was performed to evaluate the effects of fasting and high-fat diet. * $P < 0.05$; ** $P < 0.01$ vs. ad libitum eating on the same diet. # $P < 0.05$; ## $P < 0.01$ vs. standard diet on the same eating condition (ad libitum or fasting). Further analysis to clarify whether there were interactions between the effect of fasting and that of high-fat diet was performed as shown in supplemental Table S2. □, skeletal muscle; ■, brown adipose tissue; ▤, white adipose tissue. **B:** Body weight of wild-type (Wt) and GCA^{+/-} mice fed on standard diet (dotted lines) or high-fat diet (solid lines) after 8 weeks of age ($n = 8$). **C:** Food intake on high-fat diet ($n = 6$). **D:** Blood glucose levels determined with the glucose tolerance test ($n = 8$). □, wild type; ■, GCA^{+/-}. **E:** Total fat weight estimated from the CT images ($n = 6$). * $P < 0.05$; ** $P < 0.01$ vs. wild type on the same feeding condition. GCA^{+/-}, GCA heterozygous knockout mice.

cGK-Tg mice exhibit giant mitochondria in the skeletal muscle, associated with higher oxygen consumption. The respiratory gas analysis demonstrated that the oxygen consumption increased in the cGK-Tg mice, both when on standard diet and on the high-fat diet ($n = 6$, $P < 0.01$) (Fig. 5A). Mean oxygen consumption for 24 h of wild-type mice on standard diet was $63.5 \pm 0.3 \text{ ml} \cdot \text{min}^{-1} \cdot \text{kg body wt}^{-1}$, and that of cGK-Tg was $71.7 \pm 0.4 \text{ ml} \cdot \text{min}^{-1} \cdot \text{kg body wt}^{-1}$. The value of wild-type mice on high-fat diet decreased to $43.6 \pm 0.2 \text{ ml} \cdot \text{min}^{-1} \cdot \text{kg body wt}^{-1}$, and that of cGK-Tg was $54.1 \pm 0.5 \text{ ml} \cdot \text{min}^{-1} \cdot \text{kg body wt}^{-1}$ (Fig. 5B). The increase in oxygen consumption in cGK-Tg mice was accompanied with a significantly higher rectal temperature (Fig. 5C). The respiratory quotient showed a significant reduction in cGK-Tg mice ($n = 6$, $P < 0.01$) (Fig. 5D), and the reduction was prominent in

the light phase (data not shown), similar to the case of BNP-Tg mice (Fig. 2D). Fat oxidation was increased in cGK-Tg mice, both when on standard diet and on high-fat diet ($n = 6$, $P < 0.01$) (Fig. 5E). Mean fat oxidation for 24 h of high-fat-fed cGK-Tg mice was $22.8 \pm 0.5 \text{ ml} \cdot \text{min}^{-1} \cdot \text{kg body wt}^{-1}$, and that of wild-type mice was $16.8 \pm 0.3 \text{ ml} \cdot \text{min}^{-1} \cdot \text{kg body wt}^{-1}$.

Quantitative PCR analysis revealed increased mitochondrial DNA copy number in both the brown adipose tissue and the skeletal muscle of cGK-Tg mice, both on standard and high-fat diet (Fig. 5F). In conjunction with these findings, the expressions of the genes encoding PGC-1 α and UCP1 were upregulated in the brown adipose tissue of cGK-Tg mice (Fig. 5G). In the skeletal muscle, expressions of the genes encoding PGC-1 α and PPAR δ were upregulated in cGK-Tg mice, both when on standard and high-fat diet, associated with the

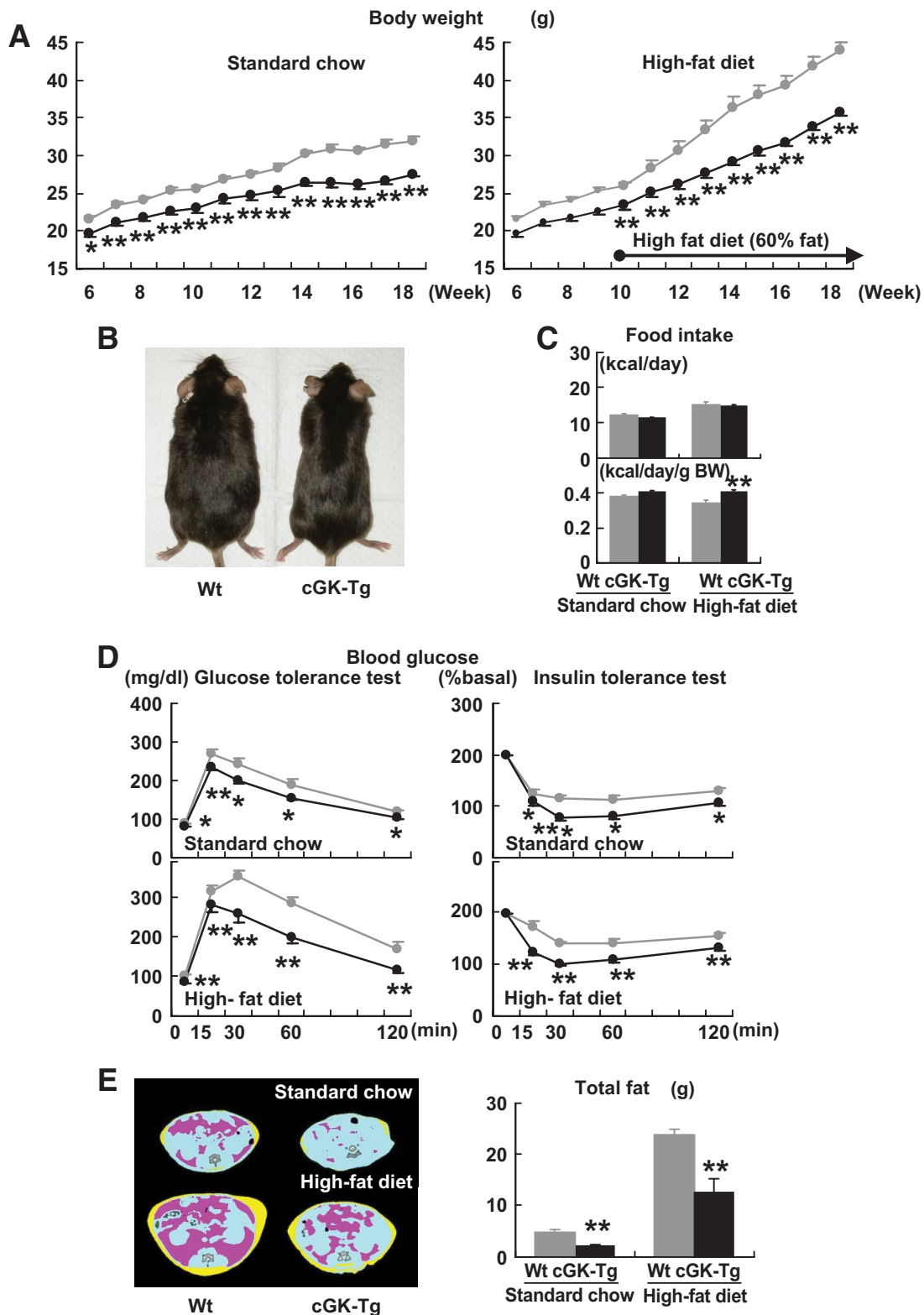


FIG. 4. cGK-Tg mice are lean and insulin sensitive even on standard diet. Wild-type and cGK-Tg mice were given a high-fat (60 kcal% fat) diet from the age of 10 weeks. **A:** Body weight of cGK-Tg mice on standard diet (*left panel*) and high-fat diet (*right panel*) ($n = 8-10$). □, wild type; ■, cGK-Tg. **B:** Macroscopic appearance of a wild-type (Wt) and a cGK-Tg mouse. **C:** Food intake on standard and high-fat diet (*upper panel*) (kcal/day, $n = 6$) and the body weight (BW)-adjusted value (*lower panel*) ($\text{kcal} \cdot \text{day}^{-1} \cdot \text{g body wt}^{-1}$). **D:** Blood glucose levels determined with the glucose and insulin tolerance tests for each genotype on standard diet and high-fat diet ($n = 8$). □, wild type; ■, cGK-Tg. **E:** CT images obtained at kidney level of a wild-type (Wt) and a cGK-Tg mouse on standard diet (*upper panel*) and high-fat diet (*lower panel*). Subcutaneous fat (yellow), abdominal fat (red), and muscular region (blue) were distinguished. Total fat weight was estimated from the images ($n = 6$). **F:** Microscopic analysis using hematoxylin and eosin staining of epididymal fats in high-fat-fed mice. Scale bar, 100 μm . **G:** Distribution of adipocyte diameter determined with Coulter counter ($n = 8$). □, wild type; ■, cGK-Tg. **H:** Macroscopic appearance of the liver in high-fat-fed mice (*upper panel*). Microscopic images with Oil red O staining of the liver (*lower panel*). Scale bar, 100 μm . **I** and **J:** Triglyceride concentration in the liver (**I**) and the quadriceps (**J**) ($n = 12$). * $P < 0.05$; ** $P < 0.01$ vs. wild type on the same feeding condition. (A high-quality color digital representation of this figure is available in the online issue.)

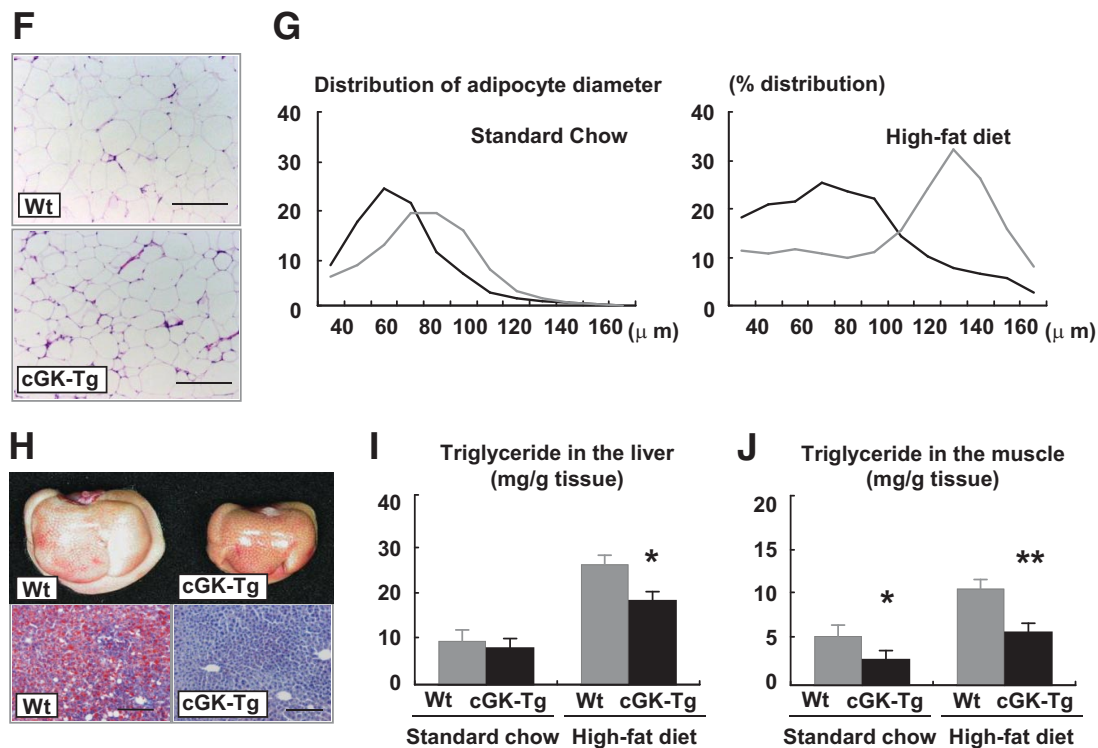


FIG. 4. Continued.

increase in their downstream target genes involved in mitochondrial oxidative function and fatty acid catabolism (Fig. 5H). In addition to PGC-1 α and PPAR δ , the expression of ATP synthase (ATPsyn), cytochrome c oxidase (COX), and carnitine palmitoyl transferase (CPT) 1b was significantly enhanced in the skeletal muscle of cGK-Tg mice, compared with wild-type mice, both when on standard diet and high-fat diet; while UCP3, fatty acid transporter (FATP), and acyl-CoA oxidase (ACO) were upregulated when on the high-fat diet only (Fig. 5H). The expression of PPAR α in the skeletal muscle of cGK-Tg mice was not significantly different from

wild-type mice, although high-fat diet increased the expression (data not shown). Giant mitochondria were densely packed in the skeletal muscle of high-fat-fed cGK-Tg mice when it was observed by means of an electron microscope (Fig. 5I).

NPs directly increase the expression of PGC-1 α and PPAR δ and mitochondrial content in cultured myocytes. The results of the study shown in Fig. 6A and B are described in supplement 2. Schematic representation of the suggested roles for NP/cGK cascades, as described in the present and previous studies, is shown in Fig. 6C.

TABLE 2

Physical and metabolic parameters of cGK-Tg mice fed on standard chow or high-fat diet

	Standard chow		High-fat diet	
	Wild type	cGK-Tg	Wild type	cGK-Tg
Body weight (g)				
18 weeks old	32.0 \pm 0.6	27.6 \pm 0.4*	43.9 \pm 1.2	35.7 \pm 1.4*
Glucose (mg/dl)				
Ad libitum feeding	160.7 \pm 6.0	137.7 \pm 5.1*	233.5 \pm 17.1	174.0 \pm 7.7*
24-h fasting	93.5 \pm 4.7	78.8 \pm 2.3 \dagger	113.5 \pm 7.6	89.8 \pm 3.7 \dagger
Insulin (ng/dl)				
Ad libitum feeding	1.4 \pm 0.2	0.8 \pm 0.2 \dagger	9.1 \pm 1.0	3.5 \pm 0.6*
24-h fasting	0.26 \pm 0.05	0.23 \pm 0.03	0.95 \pm 0.22	0.41 \pm 0.05 \dagger
Triglyceride (mg/dl)				
Ad libitum feeding	103.3 \pm 10.1	89.2 \pm 7.0	134.9 \pm 11.5	134.9 \pm 15.8
24-h fasting	84.3 \pm 6.8	81.6 \pm 6.9	112.8 \pm 9.5	103.4 \pm 11.6
Fatty acid (mEq/l)				
Ad libitum feeding	1.04 \pm 0.05	0.84 \pm 0.10	1.32 \pm 0.18	1.08 \pm 0.11
24-h fasting	1.69 \pm 0.09	1.86 \pm 0.08	1.66 \pm 0.09	2.22 \pm 0.08*
Epinephrine (ng/day)				
Urinary excretion	48.2 \pm 9.3	52.7 \pm 12.8	49.6 \pm 6.3	40.5 \pm 6.1
Norepinephrine (ng/day)				
Urinary excretion	312.3 \pm 62.2	312.3 \pm 97.4	547.7 \pm 62.2	570.3 \pm 47.6

* $P < 0.01$, $\dagger P < 0.05$ compared with wild type on the same feeding condition.

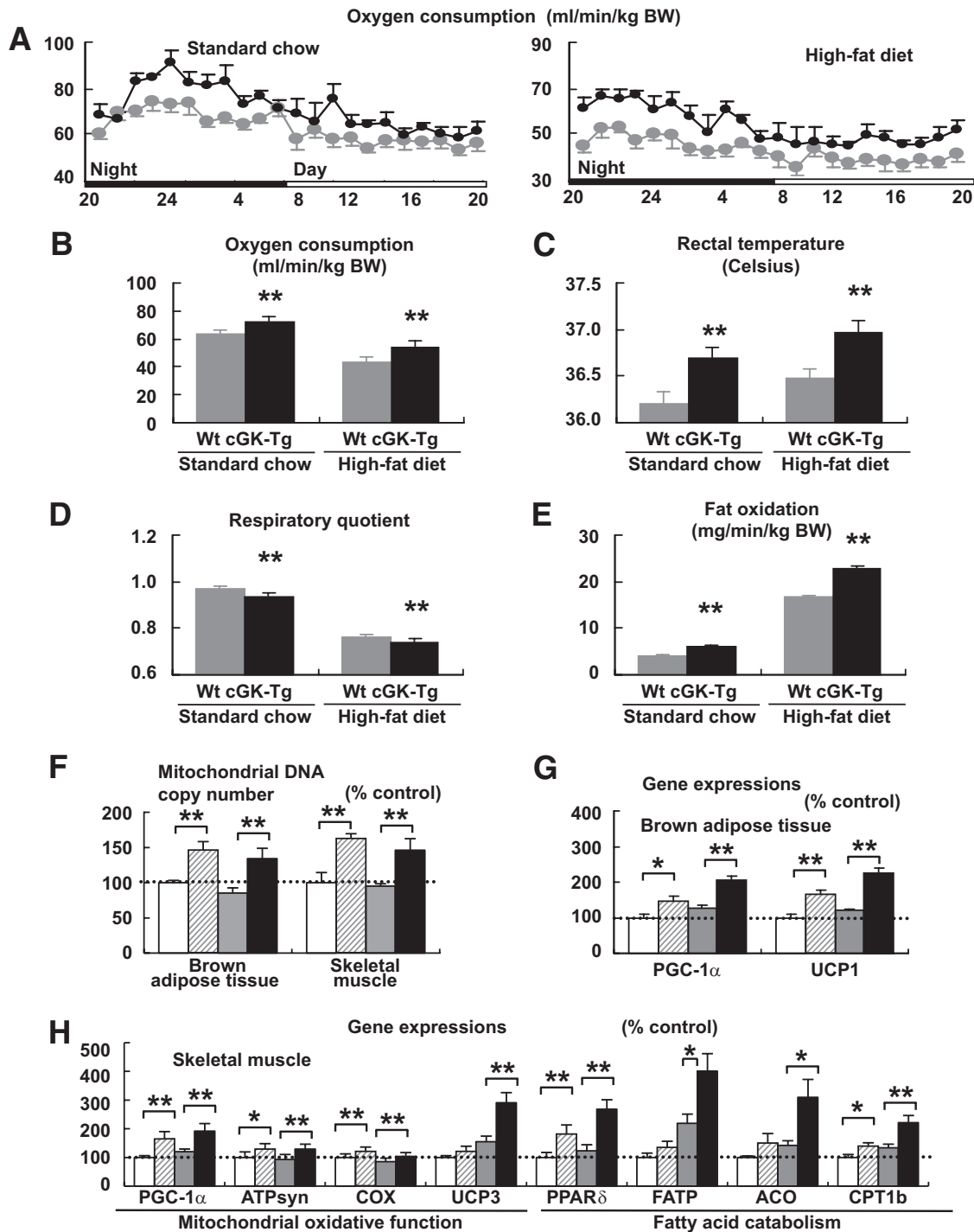


FIG. 5. cGK-Tg mice exhibit giant mitochondria in the skeletal muscle, associated with higher oxygen consumption and fat oxidation. Mice were subjected to respiratory gas analysis after fed on high-fat diet. Total DNA and RNA were extracted from the brown adipose tissue and the quadriceps, and quantitative PCR analysis was performed. *A*: Oxygen consumption on standard diet ($n = 6$). □, wild type; ■, cGK-Tg. *B*: Mean oxygen consumption for 24 h on standard or high-fat diet. *C*: Rectal temperature on standard or high-fat diet ($n = 12$). *D*: Mean respiratory quotient for 24 h on standard or high-fat diet ($n = 6$). *E*: Mean fat oxidation estimated from the respiratory gas analysis for 24 h on standard or high-fat diet ($n = 6$). *F*: Mitochondrial DNA copy number estimated from quantification of mitochondrial and nuclear genome ($n = 8$). *G*: Expressions of genes encoding PGC-1 α and UCP1 in the brown adipose tissue. The values were standardized to those for the control (wild-type [Wt] mice fed on standard diet) in either group ($n = 12$). *H*: Expressions of the genes involved in mitochondrial regulation or fatty acid catabolism in the skeletal muscle ($n = 12$). Standard diet: □, wild type (control); ▨, cGK-Tg. High-fat diet: □, wild type; ■, cGK-Tg. *I*: Electron microscopic analysis of muscle mitochondria of high-fat-fed cGK-Tg mice. * $P < 0.05$; ** $P < 0.01$ vs. wild-type mice on the same feeding condition.

DISCUSSION

The findings in this study demonstrate that the activation of NP/cGK cascades augments mitochondrial biogenesis and fat oxidation in mice through upregulation of PGC-1 α and PPAR δ in the skeletal muscle, thus conferring resis-

tance to obesity and glucose intolerance. BNP-Tg mice fed a high-fat diet were protected from obesity and insulin resistance, while cGK-Tg mice were lean even on standard diet and showed increased insulin sensitivity, and, surprisingly, giant mitochondria were densely packed in the

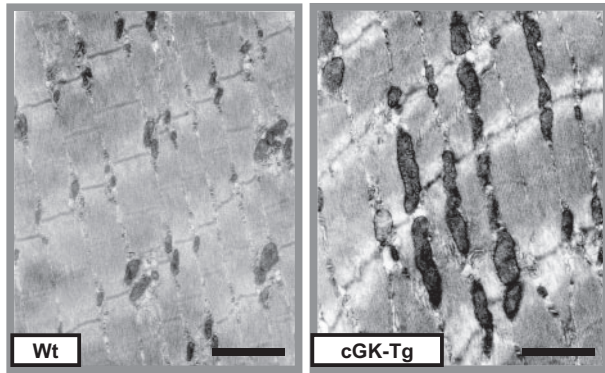


FIG. 5. Continued.

skeletal muscle. Both types of mice showed a reduction in fat tissue and excessive lipid accumulation in the liver and skeletal muscle, in accordance with an increase in fat oxidation. Functional NP receptors were upregulated during fasting, whereas they were downregulated by ad libitum feeding or high-fat challenge, while whole-body knockdown of the functional receptor, GCA, led to promotion of obesity in mice. These findings, together with those that demonstrated NP-induced lipolysis, lead us to propose the concept that NP/cGK cascades play significant roles in lipid catabolism during fasting or chronic caloric restriction, in addition to their well-known roles in the cardiovascular system, such as in the attenuation of hypertension and congestive heart failure (Fig. 6C) (7,8,17).

Genetic overexpression of NP/cGK in mice attenuated diet-induced obesity and insulin resistance, associated with the increase in muscle mitochondrial content and fat oxidation. We identified the dual upregulation of PGC-1 α and PPAR δ in the skeletal muscle of the Tg mice as a molecular basis of the increase in mitochondria and confirmed the direct increase in the expression of PGC-1 α and PPAR δ and mitochondrial content by both ANP and BNP through the experiments using cultured myocytes. PGC-1 α is a transcriptional cofactor that acts as a master regulator of mitochondrial biogenesis (18). PPAR δ is a transcription factor that binds with PGC-1 α and enhances mitochondrial biogenesis and lipid catabolism (19). Activation of PPAR δ in mice by the treatment with the PPAR δ agonist GW501516 or overexpression of a constitutively active form of PPAR δ were shown to increase muscle mitochondrial content and fatty acid oxidation and, thus, prevent diet-induced obesity and glucose intolerance (20,21). However, mice with muscle-specific overexpression of wild-type PPAR δ did not exhibit such a prominent phenotype (22). Muscle-specific overexpression of PGC-1 α has been reported to not prevent diet-induced obesity and insulin resistance in mice, although there was an increase in mitochondrial content (23). These results indicate that the coordinated increase in the expression of PGC-1 α and PPAR δ , which was observed in the skeletal muscle of BNP- and cGK-Tg mice, led to synergistic effects that were beneficial for ameliorating diet-induced obesity and insulin resistance. The expression of PGC-1 α and PPAR δ in muscle is augmented by exercise via exercise-sensitive molecules such as AMP-activated protein kinase (AMPK) (18,19). The increases in circulating NP and cGMP levels during exercise have been demonstrated in previous reports (24,25). Therefore, we hypothesize that NP/cGMP/cGK cascades can interact with the exercise-sensitive

molecules in muscle and increase the expression of PGC-1 α and PPAR δ .

BNP-Tg mice gained less body weight than controls when they were fed on high-fat diet. The same tendency was observed even when on standard diet; however, the magnitude of the change was not so prominent. We interpret the results as the Tg mice escaped from diet-induced obesity by increasing muscle mitochondrial content and fat oxidation. The elevation of serum adiponectin levels observed in the high-fat-fed BNP-Tg mice, associated with reduced adiposity, might be contributing to the attenuation of insulin resistance (26,27). Apparent changes in food intake and catecholamine kinetics were not observed.

In cGK-Tg mice, the increase in mitochondria was evident even on standard diet, resulting in the Tg mice being leaner and more insulin sensitive than BNP-Tg mice. Our data suggested that one reason for the difference in the magnitude of the altered phenotypes between the BNP- and cGK-Tg mice was caused by the variations of the target tissues. In the skeletal muscle, similar changes in gene expression were evident in the two lines of Tg mice, including upregulation of PGC-1 α and PPAR δ . In the brown adipose tissue, on the other hand, the increase in the expression level of PGC-1 α and its downstream effector UCP1 was significant in cGK-Tg mice, associated with higher body temperature; however, these changes were not so prominent in BNP-Tg mice. We observed that the functional receptors for NP, GCA, and GCB were abundantly expressed in the brown adipose tissue; however, the clearance receptor (C-receptor) was also rich in the tissue. Therefore, the functional receptor-to-C-receptor ratio, which is suggested to correlate with the biological action of NPs, was lower in the brown adipose tissue than skeletal muscle. We speculate that the abundant expression of C-receptor and the lower ratio of the functional receptors reduced the effect of NP in the brown adipose tissue.

High-fat-fed GCA heterozygous knockout mice accumulated more fat mass and were glucose intolerant compared with wild-type mice. This phenotype is the opposite to that of BNP-Tg or cGK-Tg mice so that the effects of NPs in terms of the prevention of diet-induced obesity and insulin resistance seemed to be mediated at least in part by GCA. We were unable to determine whether GCB also participated because GCB knockout mice were not available. The NP receptors were regulated by dietary conditions; that is, GCA and GCB were upregulated by fasting and downregulated during high-fat feeding. On the other hand, the C-receptor showed opposite kinetics. Therefore, the ratio of functional receptors to C-receptor was lowered by feeding or during chronic high-fat diet; conversely, fasting increased relative amount of the functional receptors. These results indicate that a high-fat diet can contribute to the development of diet-induced obesity and insulin resistance at least partly by downregulation of GCA and upregulation of the C-receptor. The notion that the kinetics of NP receptor expression depend on dietary conditions, such as high-fat diet or fasting, is consistent with earlier findings of others. The GCA-to-C-receptor ratio was shown to be lowered in obese people than in non-obese (28). Natriuresis is known to be increased after several hours of fasting, despite the fact that sodium intake is decreased (29). The upregulation of functional NP receptors in renal tubular cells by fasting and subsequent augmentation of natriuresis might account for the

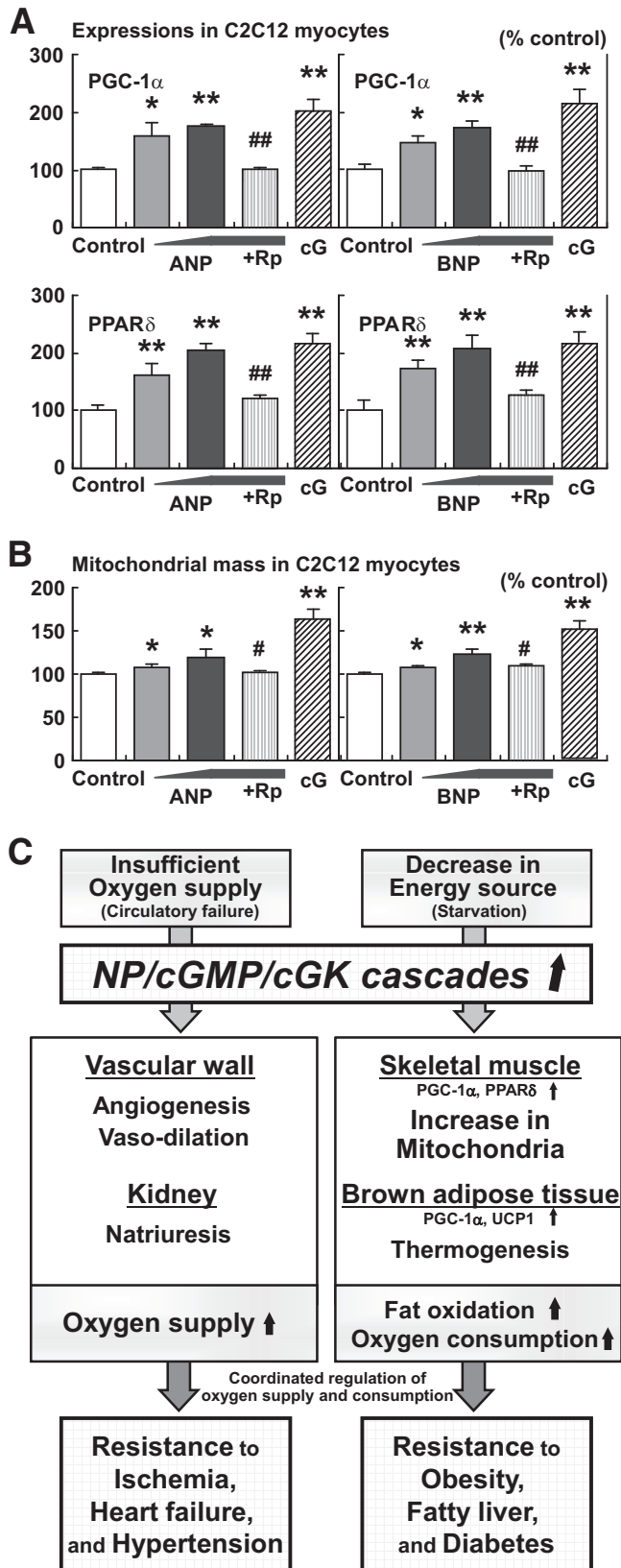


FIG. 6. NPs directly increase the expression of PGC-1 α and PPAR δ and mitochondrial content in cultured myocytes. C2C12 myocytes were stimulated with the indicated agents for 8 (A) or 48 (B) hours (ANP 10^{-11} – 10^{-9} mol/l or BNP 10^{-11} – 10^{-9} mol/l, with or without the cGMP antagonist, Rp-8-br-cGMP [Rp] 10^{-4} mol/l). Stimulation of cGK by 8-Br-cGMP (cG) 10^{-4} mol/l was also challenged ($n = 12$). A: Gene expressions of PGC-1 α and PPAR δ in C2C12 cells when treated with ANPs or BNPs. B: Mitochondrial mass in C2C12 cells quantified by use

well-known phenomenon of “fasting-induced natriuresis.” Taken together, the dietary regulation of the receptor expressions indicates that the signal transduction through NP/cGK cascades, which is augmented by starvation, might have a role in fasting-induced fat oxidation under physiological conditions.

Augmented production of NPs caused by congestive heart failure plays important roles in compensating for the volume expansion and subsequent decrease in oxygen supply by exerting vasodilating, natriuretic, and neurohumoral-modulating actions (30). This compensatory effect in the cardiovascular system has been thought to be the primary role for NP/cGK cascades (31). In the present study, we reveal the new roles for the cascades on mitochondrial biogenesis and fat oxidation through upregulation of PGC-1 α and PPAR δ . The results of the present study are in line with earlier publications from Lafontan and colleagues (6,7,32,33), which have demonstrated the importance of the NP/cGK system in the regulation of adipose tissue lipolysis. Their results and ours together support the view that NP/cGK cascades have significant roles in lipid catabolism. Moreover, the increase in circulating NP and cGMP levels during exercise has been demonstrated in previous reports (24,25). Therefore, NP/cGMP/cGK cascades might have significant roles in metabolic adaptations in response to exercise, including mitochondrial biogenesis and fat oxidation.

Several other vascular hormones that regulate vascular tone, including catecholamines, angiotensin II, and NO, are also implicated in the regulation of cellular metabolism and subsequent change in body weight and glucose tolerance (34–38). In this context, vascular hormones seem to lie at the crossroad of cardiovascular and metabolic diseases. In a recent report (9), the number of risk factors acting as diagnostic markers of metabolic syndrome is shown to inversely correlate with plasma concentrations of NPs. The clinical data and the findings of the present study collectively indicate that insufficient activation of NP/cGK cascades can be a causative factor of both obesity and hypertension. We speculate that the state of overnutrition would downregulate functional NP receptors as to promote both obesity and hypertension. Furthermore, we believe that physiological responses of vascular hormones, in accordance with blood pressure, circulating fluid volume, and oxygen demand, would result in coordinated regulation of oxygen supply and consumption, and the coordination is especially important for the adaptive responses to exercise.

To summarize, the results of the present study indicate that NP/cGK cascades can promote muscle mitochondrial biogenesis and fat oxidation through upregulation of PGC-1 α and PPAR δ , as to prevent obesity and glucose intolerance. The results were compatible with our recent report (10), which showed that cGMP can increase mitochondrial content and function in cultured myocytes. The pharmaceutical interventions that activate NP/cGMP/cGK

of MitoTracker Green, a fluorescent probe for mitochondria. * $P < 0.05$; ** $P < 0.01$ vs. control; # $P < 0.05$; ## $P < 0.01$ vs. the NP (10^{-9} mol/l)-treated group. Rp, Rp-8-br-cGMP (cGMP antagonist), cG, 8-Br-cGMP (membrane-permeable cGMP analog). C: Schematic representation of the suggested roles for NP/cGK cascades. Previous studies have shown the significant roles for NP/cGK cascades in the cardiovascular system that lead to resistance to ischemia, heart failure, and hypertension. In the present study, NP/cGK cascades are suggested to promote muscle mitochondrial biogenesis and fat oxidation, as to prevent obesity, fatty liver, and glucose intolerance.

cascades seem to be potentially beneficial for the treatment of obesity, fatty liver, and glucose intolerance.

ACKNOWLEDGMENTS

This work was supported by grants from Japanese Ministry of Education, Culture, Sports, Science, and Technology; the Ministry of Health, Labor, and Welfare; the University of Kyoto 21st Century Centers of Excellence Program; and grants from the Takeda Medical Research Foundation and the Smoking Research Foundation. The funders had no role in study design, data collection and analysis, decision to publish, or preparation of the manuscript.

No potential conflicts of interest relevant to this article were reported.

K.M. designed the experiments, maintained the mice, performed the experiments, analyzed the data, and wrote the article. H.I. directed the study, contributed to discussion, and edited the manuscript. H.T. supported the study with superb technical assistances and contributed to discussion. N.T., Y.F., M.S., K.Y., D.T., M.I., and T.S. contributed to discussion. K.N. contributed to discussion and encouraged the authors.

We thank T. Shibakusa, K. Inoue, and T. Fushiki in Kyoto University Graduate School of Agriculture and T. Nakamura and H. Sakaue in Kobe University Graduate School of Medicine for technical assistance.

GenBank accession numbers were PGC-1 α , NM_008904; PPAR δ , NM_011145; UCP1, NM_009463; ATPsyn, NM_007505; COX, NM_009941; UCP3, NM_009464; FATP, NM_011977; ACO, NM_015729; and CPT1b, NM_009948.

REFERENCES

- Potter LR, Abbey-Hosch S, Dickey DM. Natriuretic peptides, their receptors, and cyclic guanosine monophosphate-dependent signaling functions. *Endocr Rev* 2006;27:47–72
- Colucci WS, Elkayam U, Horton DP, Abraham WT, Bourge RC, Johnson AD, Wagoner LE, Givertz MM, Liang CS, Neibaur M, Haught WH, LeJemtel TH. Intravenous nesiritide, a natriuretic peptide, in the treatment of decompensated congestive heart failure. Nesiritide Study Group. *N Engl J Med* 2000;343:246–253
- Yamahara K, Itoh H, Chun TH, Ogawa Y, Yamashita J, Sawada N, Fukunaga Y, Sone M, Yurugi-Kobayashi T, Miyashita K, Tsujimoto H, Kook H, Feil R, Garbers DL, Hofmann F, Nakao K. Significance and therapeutic potential of the natriuretic peptides/cGMP/cGMP-dependent protein kinase pathway in vascular regeneration. *Proc Natl Acad Sci USA* 2003;100:3404–3409
- Park K, Itoh H, Yamahara K, Sone M, Miyashita K, Oyama N, Sawada N, Taura D, Inuzuka M, Sonoyama T, Tsujimoto H, Fukunaga Y, Tamura N, Nakao K. Therapeutic potential of atrial natriuretic peptide administration on peripheral arterial diseases. *Endocrinology* 2008;149:483–491
- Yasoda A, Komatsu Y, Chusho H, Miyazawa T, Ozasa A, Miura M, Kurihara T, Rogi T, Tanaka S, Suda M, Tamura N, Ogawa Y, Nakao K. Overexpression of CNP in chondrocytes rescues achondroplasia through a MAPK-dependent pathway. *Nat Med* 2004;10:80–86
- Sengenès C, Berlan M, De Glisezinski I, Lafontan M, Galitzky J. Natriuretic peptides: a new lipolytic pathway in human adipocytes. *FASEB J* 2000;14:1345–1351
- Sengenès C, Bouloumie A, Hauner H, Berlan M, Busse R, Lafontan M, Galitzky J. Involvement of a cGMP-dependent pathway in the natriuretic peptide-mediated hormone-sensitive lipase phosphorylation in human adipocytes. *J Biol Chem* 2003;278:48617–48626
- Wang TJ, Larson MG, Levy D, Benjamin EJ, Leip EP, Wilson PW, Vasan RS. Impact of obesity on plasma natriuretic peptide levels. *Circulation* 2004;109:594–600
- Wang TJ, Larson MG, Keyes MJ, Levy D, Benjamin EJ, Vasan RS. Association of plasma natriuretic peptide levels with metabolic risk factors in ambulatory individuals. *Circulation* 2007;115:1345–1353
- Mitsuishi M, Miyashita K, Itoh H. cGMP rescues mitochondrial dysfunction induced by glucose and insulin in myocytes. *Biochem Biophys Res Commun* 2008;367:840–845
- Ogawa Y, Itoh H, Tamura N, Suga S, Yoshimasa T, Uehira M, Matsuda S, Shiono S, Nishimoto H, Nakao K. Molecular cloning of the complementary DNA and gene that encode mouse brain natriuretic peptide and generation of transgenic mice that overexpress the brain natriuretic peptide gene. *J Clin Invest* 1994;93:1911–1921
- Lopez MJ, Wong SK, Kishimoto I, Dubois S, Mach V, Friesen J, Garbers DL, Beuve A. Salt-resistant hypertension in mice lacking the guanylyl cyclase-A receptor for atrial natriuretic peptide. *Nature* 1995;378:65–68
- Sakai T, Sakaue H, Nakamura T, Okada M, Matsuki Y, Watanabe E, Hiramatsu R, Nakayama K, Nakayama KI, Kasuga M. Skp2 controls adipocyte proliferation during the development of obesity. *J Biol Chem* 2007;282:2038–2046
- Shibakusa T, Mizunoya W, Okabe Y, Matsumura S, Iwaki Y, Okuno A, Shibata K, Inoue K, Fushiki T. Transforming growth factor-beta in the brain is activated by exercise and increases mobilization of fat-related energy substrates in rats. *Am J Physiol Regul Integr Comp Physiol* 2007;292:R1851–R1861
- Jequier E, Acheson K, Schutz Y. Assessment of energy expenditure and fuel utilization in man. *Annu Rev Nutr* 1987;7:187–208
- Lagouge M, Argmann C, Gerhart-Hines Z, Meziane H, Lerin C, Daussin F, Messadeq N, Milne J, Lambert P, Elliott P, Geny B, Laakso M, Puigserver P, Auwerx J. Resveratrol improves mitochondrial function and protects against metabolic disease by activating SIRT1 and PGC-1 α . *Cell* 2006;127:1109–1122
- Itoh H, Nakao K, Mukoyama M, Yamada T, Hosoda K, Shirakami G, Morii N, Sugawara A, Saito Y, Shiono S, Arai H, Yoshida I, Imura H. Chronic blockade of endogenous atrial natriuretic polypeptide (ANP) by monoclonal antibody against ANP accelerates the development of hypertension in spontaneously hypertensive and deoxycorticosterone acetate-salt-hypertensive rats. *J Clin Invest* 1989;84:145–154
- Lin J, Handschin C, Spiegelman BM. Metabolic control through the PGC-1 family of transcription coactivators. *Cell Metab* 2005;1:361–370
- Barish GD, Narkar VA, Evans RM. PPAR δ : a dagger in the heart of the metabolic syndrome. *J Clin Invest* 2006;116:590–597
- Wang YX, Zhang CL, Yu RT, Cho HK, Nelson MC, Bayuga-Ocampo CR, Ham J, Kang H, Evans RM. Regulation of muscle fiber type and running endurance by PPAR δ . *PLoS Biol* 2004;2:e294
- Tanaka T, Yamamoto J, Iwasaki S, Asaba H, Hamura H, Ikeda Y, Watanabe M, Magoori K, Ioka RX, Tachibana K, Watanabe Y, Uchiyama Y, Sumi K, Iguchi H, Ito S, Doi T, Hamakubo T, Naito M, Auwerx J, Yanagisawa M, Kodama T, Sakai J. Activation of peroxisome proliferator-activated receptor delta induces fatty acid beta-oxidation in skeletal muscle and attenuates metabolic syndrome. *Proc Natl Acad Sci USA* 2003;100:15924–15929
- Luquet S, Lopez-Soriano J, Holst D, Fredenrich A, Melki J, Rassoulzadegan M, Grimaldi PA. Peroxisome proliferator-activated receptor delta controls muscle development and oxidative capability. *FASEB J* 2003;17:2299–2301
- Choi CS, Befroy DE, Codella R, Kim S, Reznick RM, Hwang YJ, Liu ZX, Lee HY, Distefano A, Samuel VT, Zhang D, Cline GW, Handschin C, Lin J, Petersen KF, Spiegelman BM, Shulman GI. Paradoxical effects of increased expression of PGC-1 α on muscle mitochondrial function and insulin-stimulated muscle glucose metabolism. *Proc Natl Acad Sci USA* 2008;105:19926–19931
- Moro C, Crampes F, Sengenès C, De Glisezinski I, Galitzky J, Thalamas C, Lafontan M, Berlan M. Atrial natriuretic peptide contributes to physiological control of lipid mobilization in humans. *FASEB J* 2004;18:908–910
- Ruskoaho H, Kinnunen P, Taskinen T, Vuolteenaho O, Leppälouo J, Takala TE. Regulation of ventricular atrial natriuretic peptide release in hypertrophied rat myocardium: effects of exercise. *Circulation* 1989;80:390–400
- Arita Y, Kihara S, Ouchi N, Takahashi M, Maeda K, Miyagawa J, Hotta K, Shimomura I, Nakamura T, Miyaoka K, Kuriyama H, Nishida M, Yamashita S, Okubo K, Matsubara K, Muraguchi M, Ohmoto Y, Funahashi T, Matsuzawa Y. Paradoxical decrease of an adipose-specific protein, adiponectin, in obesity. *Biochem Biophys Res Commun* 1999;257:79–83
- Yamauchi T, Kamon J, Waki H, Terauchi Y, Kubota N, Hara K, Mori Y, Ide T, Murakami K, Tsuboyama-Kasaoka N, Ezaki O, Akanuma Y, Gavrilova O, Vinson C, Reitman ML, Kagechika H, Shudo K, Yoda M, Nakano Y, Tobe K, Nagai R, Kimura S, Tomita M, Froguel P, Kadowaki T. The fat-derived hormone adiponectin reverses insulin resistance associated with both lipodystrophy and obesity. *Nat Med* 2001;7:941–946
- Dessi-Fulgheri P, Sarzani R, Rappelli A. The natriuretic peptide system in obesity-related hypertension: new pathophysiological aspects. *J Nephrol* 1998;11:296–299
- Szénási G, Bencsáth P, Szalay L, Takács L. Fasting induces denervation natriuresis in the conscious rat. *Am J Physiol* 1985;249:F753–F758

30. Mukoyama M, Nakao K, Saito Y, Ogawa Y, Hosoda K, Suga S, Shirakami G, Jougasaki M, Imura H. Increased human brain natriuretic peptide in congestive heart failure. *N Engl J Med* 1990;323:757–758
31. Boerrigter G, Burnett JC Jr. Recent advances in natriuretic peptides in congestive heart failure. 2004. *Expert Opin Investig Drugs*. 13: 643–652
32. Moro C, Polak J, Hejnova J, Klimcakova E, Crampes F, Stich V, Lafontan M, Berlan M. Atrial natriuretic peptide stimulates lipid mobilization during repeated bouts of endurance exercise. *Am J Physiol Endocrinol Metab* 2006;290:E864–E869
33. Lafontan M, Moro C, Berlan M, Crampes F, Sengenès C, Galitzky J. Control of lipolysis by natriuretic peptides and cyclic GMP. *Trends Endocrinol Metab* 2008;19:130–137
34. Mitsuishi M, Miyashita K, Muraki A, Itoh H. Angiotensin II reduces mitochondrial content in skeletal muscle and affects glycemic control. *Diabetes* 2009;58:710–717
35. Massiera F, Seydoux J, Geloën A, Quignard-Boulange A, Turban S, Saint-Marc P, Fukamizu A, Negrel R, Ailhaud G, Teboul M. Angiotensinogen-deficient mice exhibit impairment of diet-induced weight gain with alteration in adipose tissue development and increased locomotor activity. *Endocrinology* 2001;142:5220–5225
36. Bachman ES, Dhillon H, Zhang CY, Cinti S, Bianco AC, Kobilka BK, Lowell BB. betaAR signaling required for diet-induced thermogenesis and obesity resistance. *Science* 2002;297:843–845
37. Duplain H, Burcelin R, Sartori C, Cook S, Egli M, Lepori M, Vollenweider P, Pedrazzini T, Nicod P, Thorens B, Scherrer U. Insulin resistance, hyperlipidemia, and hypertension in mice lacking endothelial nitric oxide synthase. *Circulation* 2001;104:342–345
38. Shankar RR, Wu Y, Shen HQ, Zhu JS, Baron AD. Mice with gene disruption of both endothelial and neuronal nitric oxide synthase exhibit insulin resistance. *Diabetes* 2000;49:684–687